Quantitative Finance and Economics

https://www.aimspress.com/journal/QFE

QFE, 9(2): 300–316.
DOI: 10.3934/QFE.2025010
Received: 14 January 2025
Revised: 17 March 2025
Accepted: 21 April 2025
Published: 24 April 2025

Research article

Accurate computation of Greeks for equity-linked security (ELS) near early redemption dates

Yunjae Nam[1], Changwoo Yoo[1], Hyundong Kim[2], Jaewon Hong[1], Minjoon Bang[1] and Junseok Kim[3,*]

[1] Program in Actuarial Science and Financial Engineering, Korea University, Seoul 02841, Republic of Korea

[2] Department of Mathematics and Physics, Gangneung-Wonju National University, Gangneung 25457, Republic of Korea

[3] Department of Mathematics, Korea University, Seoul 02841, Republic of Korea

* **Correspondence:** Email: cfdkim@korea.ac.kr.

Abstract: This study presents a numerical method for accurately computing the option values and Greeks of equity-linked securities (ELS) near early redemption dates. The Black–Scholes (BS) equation is solved using the finite difference method (FDM), and a Dirichlet boundary condition is applied at strike prices instead of directly replacing option values above the strike price with predefined option prices. This approach improves the accuracy of option pricing, particularly in the presence of early redemption structures. The proposed method is demonstrated to be effective in computing Greeks, which are crucial for risk management and hedging strategies in ELS markets. The computational tests validate the reliability of the method in capturing the sensitivities of ELS prices to various market factors.

Keywords: Equity-linked securities; Greeks; Finite difference method

JEL Codes: C63, G13, G12

1. Introduction

The step-down equity-linked security (ELS) is a structured investment instrument where the coupon or interest rate paid to investors increases over time based on predefined conditions, frequently tied to the performance of a specific equity index or stock (Jo and Kim, 2013).

Since the fourth quarter of 2022, Korean financial regulators have been directing Hang Seng China Enterprises Index (HSCEI, H-index)-based ELS sellers (5 banks, 7 securities companies) to establish

a customer response system to prepare for potential investor losses following the sharp decline in the H-index. The problematic product is mainly ELS issued since early 2021, when the H-index was at its peak, and given the recent trend of the H-index, investor losses are likely to occur from early 2024, when the ELS will mature.

It is necessary to compute the Greeks of ELS and proceed with the overall interpretation so that we can prepare for these risks. Greeks computations, which refer to the measures of risk derived from options pricing models, are important in step-down ELS derivatives. Through Greek values, we can interpret the sensitivity of step-down ELS to fluctuations in factors like the underlying asset price, maturity, volatility, and interest rate. When designing step-down ELS, issuers use Greek computations to determine the optimal structure of the product to meet the desired risk-return profile. By incorporating Greeks into pricing models, market participants can estimate the fair value of the product under different market scenarios and assess its attractiveness relative to alternative investments.

Meanwhile, ongoing numerical investigations have been conducted and continue to be actively pursued to price the fair value of an ELS derivative with a step-down structure composed of multiple underlying assets. Wu et al. (2023) studied step-down ELS options under the fractional BS model, which incorporates long-term stock correlations. They revealed that higher Hurst exponents increase repayment returns in multi-asset ELS. Cui et al. (2024) proposed the step-down ELS evaluation by applying a unified pricing framework with continuous-time Markov chain approximation and employed stochastic gradient descent to minimize the stochastic local volatility of hedging loss under various asset models. Lee et al. (2024) studied evaluating step-down ELS by applying logistic regression with the Monte Carlo method from Hwang et al. (2023) to predict exit probabilities in a multi-dimensional Brownian bridge. This approach demonstrates the efficiency of numerically estimating the exit and co-exit probabilities, which enables effective pricing of complex structured products.

In this study, we introduce a computational method for the accurate computation of the option prices and Greeks for ELS near early redemption dates. We consider the price of an ELS option with one asset. The parameters are set as follows: maturity time T, the computational domain $\Omega = (0, 300)$, strike prices $[K_1, K_2, K_3, K_4, K_5, K_6]$, coupon rates $[c_1, c_2, c_3, c_4, c_5, c_6]$, knock-in barrier D, dummy rate $d = F(1 + c_6)$ with face value F, and stock price S_0. The strike prices are arranged as $K_1 \geq K_2 \geq K_3 \geq K_4 \geq K_5 \geq K_6$, and the coupon rates set as $c_1 \leq c_2 \leq c_3 \leq c_4 \leq c_5 \leq c_6$ for each early redemption date $T_1 \leq T_2 \leq T_3 \leq T_4 \leq T_5 \leq T_6$.

Two option prices $v(S, t)$ and $u(S, t)$ can be defined through the equation solved numerically, corresponding to whether the knock-in barrier is hit or not. If the knock-in barrier is touched, the payoff of ELS is as follows:

$$v(S, T_i) = \begin{cases} F(1 + c_6), & \text{if } S \geq K_6, \\ FS/S_0, & \text{otherwise.} \end{cases} \tag{1}$$

In more detail, the payoff scenario when the knock-in barrier is touched is shown in Figure 1 (①, ②, ③, ④, ⑤, ⑥, ⑧, ⑨). In contrast, without the knock-in barrier, the payoff of ELS is given by

$$u(S, T_i) = \begin{cases} F(1 + c_6), & \text{if } S \geq K_6, \\ F(1 + d), & \text{if } D < S < K_6, \\ FS/S_0, & \text{otherwise.} \end{cases} \tag{2}$$

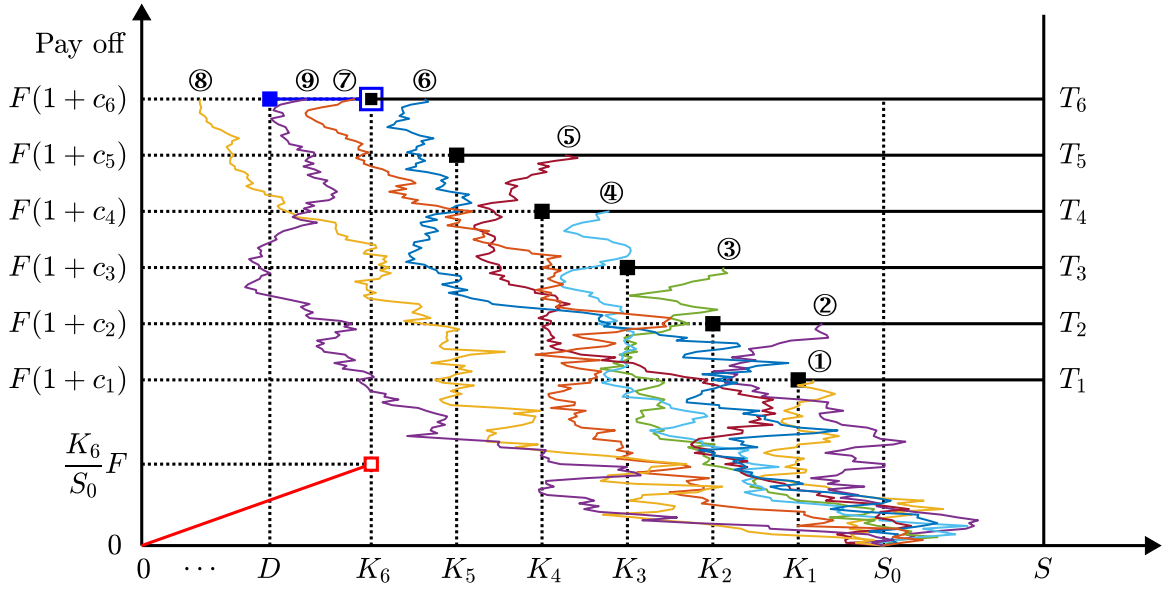

Figure 1. Function of payoff at early redemption dates.

A detailed illustration of the payoff scenario when the knock-in barrier is not breached is presented in Figure 1 (①, ②, ③, ④, ⑤, ⑥, ⑦, ⑧).

To evaluate the price of derivatives, the no-arbitrage theory in continuous time provides a fundamental framework. Under this framework, the price of the underlying asset S_t is assumed to follow a geometric Brownian motion (GBM), which is modeled by the following stochastic differential equation:

$$dS_t = rS_t dt + \sigma S_t dW_t,$$

where r represents the drift rate, σ is the volatility, and W_t is a standard Wiener process. This assumption implies that the logarithm of the asset price follows a GBM with drift, which serves as the foundation for the derivation of the BS equation. Black and Scholes (1973) formulated a partial differential equation for option pricing based on the no-arbitrage principle and the concept of a self-financing portfolio. By constructing a risk-free portfolio composed of the option and the underlying asset, the BS equation is obtained as follows:

$$\frac{\partial v(S,t)}{\partial t} + \frac{(\sigma S)^2}{2}\frac{\partial^2 v(S,t)}{\partial S^2} + rS\frac{\partial v(S,t)}{\partial S} - rv(S,t) = 0, \tag{3}$$

where $v(S,t)$ represents the option price at the underlying asset price S and time t and r is the risk-free interest rate. The BS equation is solved by imposing a terminal condition at maturity T, $v(S,T)$, along with appropriate boundary conditions.

The BS equation is a widely used method for evaluating derivatives, and various numerical methods have been developed to evaluate increasingly complex products. Liu et al. (2024) proposed a novel numerical method that employs the radial basis function-finite difference solver to approximate derivatives and solve multi dimensional option pricing problems. Roul and Goura (2020) introduced a novel numerical scheme for option pricing, utilizing the Crank–Nicolson and sextic B-spline collocation methods to solve the generalized BS equation. Tao et al. (2023) conducted a study that proposed an

Asian option pricing formula based on sub fractional Brownian motion and the sub fractional Vasicek model, analyzing its impact using the BS equation and a novel numerical scheme.

The ELS price and its Greeks are calculated through the finite difference method (FDM). The proposed algorithm solves the BS equation at early redemption dates using the Dirichlet boundary condition at strike prices instead of overwriting the option values on greater than or equal to strike prices by the given option prices.

This article is structured as follows. Section 2 describes the computational solution with FDM. Section 3 provides the values and surfaces of Greeks. In Section 4, we numerically evaluate the prices and Greeks of ELS products for different payoffs. Finally, Section 5 concludes the paper.

2. Numerical solutions

Let $\tau = T - t$. Then, Equation (3) becomes

$$\frac{\partial v(S,\tau)}{\partial \tau} = \frac{(\sigma S)^2}{2}\frac{\partial^2 v(S,\tau)}{\partial S^2} + rS\frac{\partial v(S,\tau)}{\partial S} - rv(S,\tau) \tag{4}$$

with an initial condition $v(S, 0)$. To numerically solve Equation (4), we restrict the infinite underlying domain for S into a finite domain, $[0,\ S_{\max}]$. Equation (4) is discretized using an implicit FDM with a nonuniform grid (Lee et al., 2023):

$$\begin{aligned}\frac{v_i^{n+1} - v_i^n}{\Delta\tau} &= \frac{(\sigma S_i)^2}{2}\left(\frac{2v_{i-1}^{n+1}}{h_{i-1}(h_{i-1}+h_i)} - \frac{2v_i^{n+1}}{h_{i-1}h_i} + \frac{2v_{i+1}^{n+1}}{h_i(h_{i-1}+h_i)}\right) \\ &+ rS_i\left(\frac{-h_i v_{i-1}^{n+1}}{h_{i-1}(h_{i-1}+h_i)} + \frac{(h_i - h_{i-1})v_i^{n+1}}{h_{i-1}h_i} + \frac{h_{i-1}v_{i+1}^{n+1}}{h_i(h_{i-1}+h_i)}\right) - rv_i^{n+1},\end{aligned} \tag{5}$$

where $v_i^n \equiv v(S_i, \tau_n)$, $S_{i+1} = S_i + h_i$, $S_1 = 0$, $S_{N_x} = S_{\max}$, $\tau_{n+1} = \tau_n + \Delta\tau$, and $\tau_1 = 0$. Here, h_i and $\Delta\tau$ are the step sizes of the underlying asset and time, respectively (Liu et al., 2024). We use a linear boundary condition; therefore, it is convenient to define $S_{N_x+1} = 2S_{N_x} - S_{N_x-1}$ so that the numerical second derivative at S_{N_x} is always zero and the numerical solution is linear at the right boundary. Figure 2 displays a schematic illustration of the underlying asset S.

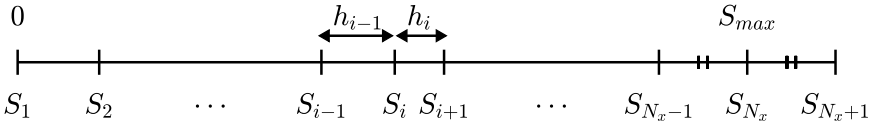

Figure 2. Schematic of discrete domain.

Equation (5) can be rewritten as follows:

$$\alpha_i v_{i-1}^{n+1} + \beta_i v_i^{n+1} + \gamma_i v_{i+1}^{n+1} = f_i,\ i = 2, \ldots, N_x, \tag{6}$$

where

$$\alpha_i = \frac{-(\sigma S_i)^2 + rS_i h_i}{h_{i-1}(h_{i-1}+h_i)},\ \beta_i = \frac{1}{\Delta\tau} + \frac{(\sigma S_i)^2 - rS_i(h_i - h_{i-1})}{h_{i-1}h_i} + r, \tag{7}$$

$$\gamma_i = \frac{-(\sigma S_i)^2 - rS_i h_{i-1}}{h_i(h_{i-1}+h_i)},\ f_i = \frac{v_i^n}{\Delta\tau}. \tag{8}$$

When early redemption is not possible, the following boundary conditions are satisfied. From the zero Dirichlet boundary condition at $i = 1$, we have $v_1^{n+1} = 0$. At $i = N_x$, we apply the linear boundary condition, $v_{N_x+1}^{n+1} = 2v_{N_x}^{n+1} - v_{N_x-1}^{n+1}$ and get

$$(\alpha_{N_x} - \gamma_{N_x})v_{N_x-1}^{n+1} + (\beta_{N_x} + 2\gamma_{N_x})v_{N_x}^{n+1} = f_{N_x}. \tag{9}$$

Then, the solution vector $v_{2:N_x}^{n+1} = [v_2^{n+1}\ v_3^{n+1}\ \cdots\ v_{N_x}^{n+1}]^T$ can be obtained by solving the tridiagonal system

$$Av_{2:N_x}^{n+1} = f_{2:N_x}, \tag{10}$$

where A is a tridiagonal matrix formed from Equation (6) with the zero Dirichlet at $i = 1$ and linear boundary conditions at $i = N_x$, That is,

$$A_{2:N_x} = \begin{pmatrix} \beta_2 & \gamma_2 & 0 & 0 & \cdots & 0 & 0 & 0 \\ \alpha_3 & \beta_3 & \gamma_3 & 0 & \cdots & 0 & 0 & 0 \\ 0 & \alpha_4 & \beta_4 & \gamma_4 & \cdots & 0 & 0 & 0 \\ \vdots & \vdots & \vdots & \vdots & \ddots & \vdots & \vdots & \vdots \\ 0 & 0 & 0 & 0 & \cdots & \alpha_{N_x-1} & \beta_{N_x-1} & \gamma_{N_x-1} \\ 0 & 0 & 0 & 0 & \cdots & 0 & \alpha_{N_x} - \gamma_{N_x} & \beta_{N_x} + 2\gamma_{N_x} \end{pmatrix}$$

and

$$f_{2:N_x} = \begin{pmatrix} f_2 \\ f_3 \\ f_4 \\ \vdots \\ f_{N_x-1} \\ f_{N_x} \end{pmatrix}.$$

Let S_{K_j} be the price of early repayment and c_j be the coupon rate of early repayment for $j = 5, \cdots, 1$. When early redemption occurs at the evaluation time, v has the Dirichlet boundary conditions at $i = 1$, we have $v_1^{n+1} = 0$ and at $i = K_j$, $v_{K_j}^{n+1} = F(1+c_j)$. Then, the solution vector $v_{2:K_j-1}^{n+1} = [v_2^{n+1}\ v_3^{n+1}\ \cdots\ v_{K_j-1}^{n+1}]^T$ can be determined by solving the tridiagonal system

$$Av_{2:K_j-1}^{n+1} = f_{2:K_j-1}, \tag{11}$$

where A is a tridiagonal matrix constructed from Equation (6) with the zero Dirichlet boundary condition at $i = 1$ and the Dirichlet boundary condition at $i = K_j$, That is,

$$A_{2:K_j-1} = \begin{pmatrix} \beta_2 & \gamma_2 & 0 & 0 & \cdots & 0 & 0 & 0 \\ \alpha_3 & \beta_3 & \gamma_3 & 0 & \cdots & 0 & 0 & 0 \\ 0 & \alpha_4 & \beta_4 & \gamma_4 & \cdots & 0 & 0 & 0 \\ \vdots & \vdots & \vdots & \vdots & \ddots & \vdots & \vdots & \vdots \\ 0 & 0 & 0 & 0 & \cdots & \alpha_{K_j-2} & \beta_{K_j-2} & \gamma_{K_j-2} \\ 0 & 0 & 0 & 0 & \cdots & 0 & \alpha_{K_j-1} & \beta_{K_j-1} \end{pmatrix}$$

and

$$f_{2:K_j-1} = \begin{pmatrix} f_2 \\ f_3 \\ f_4 \\ \vdots \\ f_{K_j-1} \\ f_{K_j} - \gamma_{K_j-1} v_{K_j}^{n+1} \end{pmatrix}.$$

We utilize the Thomas algorithm (Thomas, 1949) to solve Equations (10) and (11), which inverts the tridiagonal matrix directly.

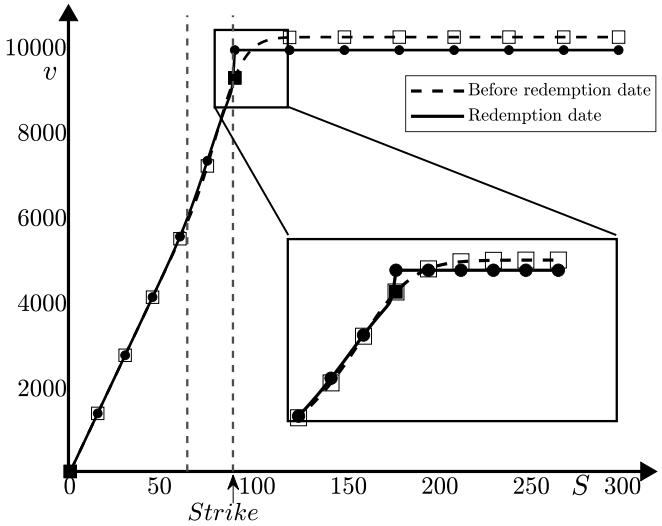

Figure 3. Option values v at before redemption date and redemption date.

First, we calculate $v(S, \tau)$. Subsequently, Figure 3 illustrates the option values v at both the pre-redemption and the redemption date. These values are then used to compute $u(S, \tau)$ by applying Dirichlet boundary conditions at the knock-in barrier. From the Dirichlet boundary condition at $i = D$ and $i = K_j$, we obtain $u_D^{n+1} = v_D^{n+1}$ and $u_{K_j}^{n+1} = F(1 + c_j)$, as shown in Figure 4.

$$\beta_{D+1} u_{D+1}^{n+1} + \gamma_{D+1} u_{D+2}^{n+1} = g_{D+1} - \alpha_{D+1} u_D^{n+1}, \tag{12}$$

$$\alpha_{K_j-1} u_{K_j-2}^{n+1} + \beta_{K_j-1} u_{K_j-1}^{n+1} = g_{K_j-1} - \gamma_{K_j-1} u_{K_j}^{n+1}. \tag{13}$$

Then, the solution vector $u_{D+1:K_j-1}^{n+1} = [u_{D+1}^{n+1} \; u_{D+2}^{n+1} \; \cdots \; u_{K_j-1}^{n+1}]^T$ can be obtained by resolving the tridiagonal system

$$B u_{D+1:K_j-1}^{n+1} = g_{D+1:K_j-1}, \tag{14}$$

where A is a tridiagonal matrix formed from similar to Equation (6) with the Dirichlet at $i = D$ and

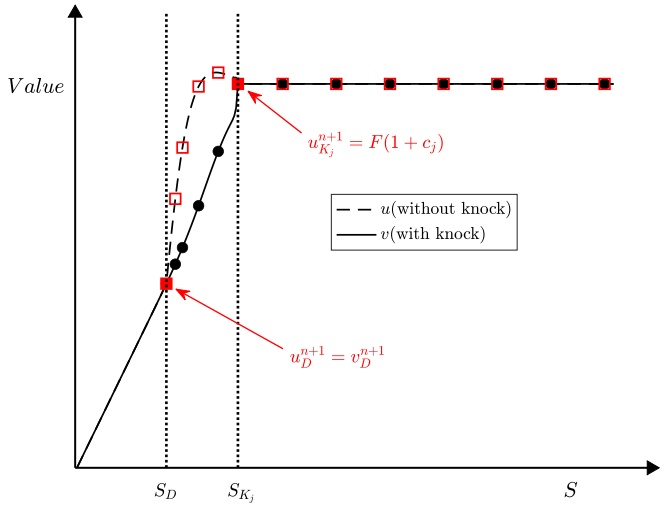

Figure 4. Option values u without knock and v with knock.

$i = K_j$, That is,

$$A_{D+1:K_j-1} = \begin{pmatrix} \beta_{D+1} & \gamma_{D+1} & 0 & 0 & \cdots & 0 & 0 & 0 \\ \alpha_{D+2} & \beta_{D+2} & \gamma_{D+2} & 0 & \cdots & 0 & 0 & 0 \\ 0 & \alpha_{D+3} & \beta_{D+3} & \gamma_{D+3} & \cdots & 0 & 0 & 0 \\ \vdots & \vdots & \vdots & \vdots & \ddots & \vdots & \vdots & \vdots \\ 0 & 0 & 0 & 0 & \cdots & \alpha_{K_j-2} & \beta_{K_j-2} & \gamma_{K_j-2} \\ 0 & 0 & 0 & 0 & \cdots & 0 & \alpha_{K_j-1} & \beta_{K_j-1} \end{pmatrix}$$

$$\text{and } f_{D+1:K_j-1} = \begin{pmatrix} f_{D+1} - \alpha_{D+1} u_D^{n+1} \\ f_{D+2} \\ f_{D+2} \\ \vdots \\ f_{K_j-2} \\ f_{K_j-1} - \gamma_{K_j-1} u_{K_j}^{n+1} \end{pmatrix}.$$

We also utilize the Thomas algorithm (Thomas, 1949) to solve Equation (11), which inverts the tridiagonal matrix (Kwak et al., 2023). Then, the option value u at the redemption date can be obtained, as illustrated in Figure 5.

3. Computational experiments

In this section, we compute the values of the Greeks for ELS and visualize their surfaces, which include delta (Δ), gamma (Γ), theta (Θ), vega (ν), and rho (ρ). Unless otherwise stated, this section uses the parameters summarized in Table 1.

The value of ELS exhibits sharp changes near the knock-in barrier and strike price due to rapid variations in the payoff. Therefore, to accurately capture these changes and minimize numerical errors, we calculate its value using a finer grid in these regions, as shown in Figure 6. This approach improves numerical accuracy by mitigating approximation errors, which can become significant when using a

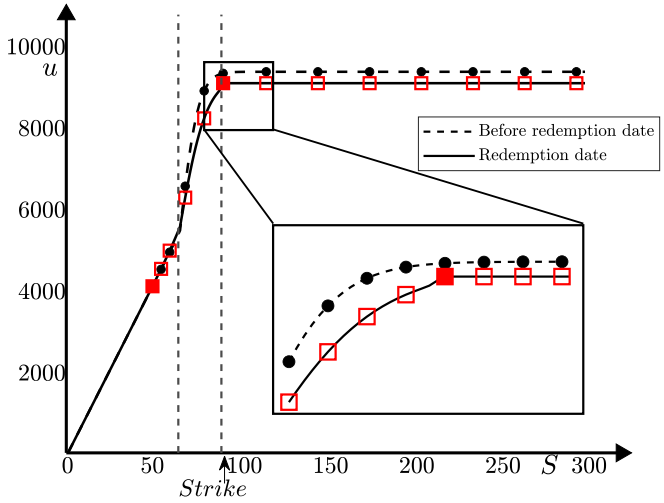

Figure 5. Option values u at before redemption date and redemption date.

Table 1. Parameters used in Section 3

Parameter	Value
Maturity time, T	3
Repayment times, $[T_1, T_2, T_3, T_4, T_5, T_6]$	$[0.5, 1, 1.5, 2, 2.5, 3]$
Time step size, $\Delta\tau$	$1/360$
Computational domain, Ω	$(0, 300)$
Current stock price, S_0	100
Strike prices, $[K_1, K_2, K_3, K_4, K_5, K_6]$	$[95, 95, 90, 90, 85, 85]$
Knock-in barrier, D	50
Coupon rates, $[c_1, c_2, c_3, c_4, c_5, c_6]$	$[0.02, 0.04, 0.06, 0.08, 0.1, 0.12]$
Dummy rate, d	0.12
Face value, F	100
Risk-free interest, r	0.03
Volatility, σ	0.2

coarse grid in areas with large changes (Lyu et al., 2021). In particular, the rapid variations in the payoff near the knock-in barrier and strike price require a finer grid for more precise approximations of derivatives, ensuring a more accurate evaluation of the option price.

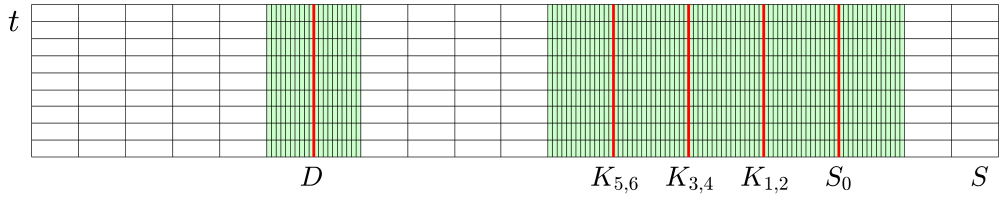

Figure 6. Non-uniform mesh grid for computational experiments.

3.1. Delta (Δ)

The variation in the value of the option due to small fluctuations in the underlying asset price is indicated by the Δ, helping issuers decide on the initial coupon rate and the step-down mechanisms based on their risk tolerance and market outlook. Moreover, Δ plays an important role in measuring the sensitivity of ELS to price, thereby helping to construct a portfolio that reduces risk (Kim et al., 2021). It can be calculated using finite difference approximations as follows.

$$\Delta_i^n = \left(\frac{\partial u}{\partial S}\right)_i^n = \frac{-h_i u_{i-1}^n}{h_{i-1}(h_{i-1}+h_i)} + \frac{(h_i - h_{i-1})u_i^n}{h_{i-1}h_i} + \frac{h_{i-1}u_{i+1}^n}{h_i(h_{i-1}+h_i)}.$$

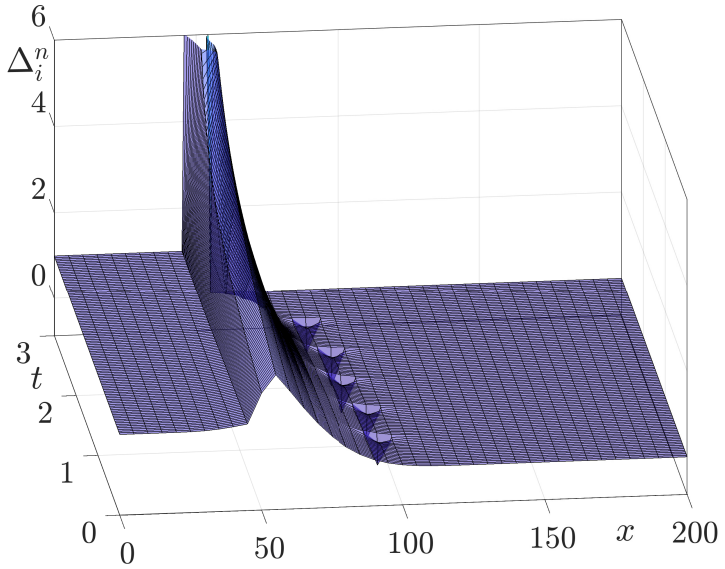

Figure 7. Δ surface of ELS at each early redemption dates and until maturity under specific conditions and its corresponding conditioned price.

Figure 7 shows the Δ surface as time and the strike price change. The Δ value increases and declines rapidly near the knock-in barrier because of Δ properties. Normally, rises as the price of the underlying asset falls and declines as the price of the underlying asset increases. The majority of ELS products currently available are step-down structures, leading to positive Δ values. Hence, it is essential to consider this and implement hedging strategies (Kanamura (2018); Larguinho et al. (2022)), such as selling the relevant underlying assets.

3.2. Gamma (Γ)

The variation of Δ is measured by Γ, which reflects the convexity of the payoff of the product. It represents the rate at which Δ changes in response to variations. Essentially, Γ is a partial differentiation of underlying assets for Δ, which is a second-order partial derivative of underlying asset with respect to options. The computation of Γ entails numerical discretization at S_i, as outlined below.

$$\Gamma_i^n = \left(\frac{\partial^2 u}{\partial S^2}\right)_i^n = 2\left(\frac{u_{i-1}^n}{h_{i-1}(h_{i-1}+h_i)} - \frac{u_i^n}{h_{i-1}h_i} + \frac{u_{i+1}^n}{h_i(h_{i-1}+h_i)}\right).$$

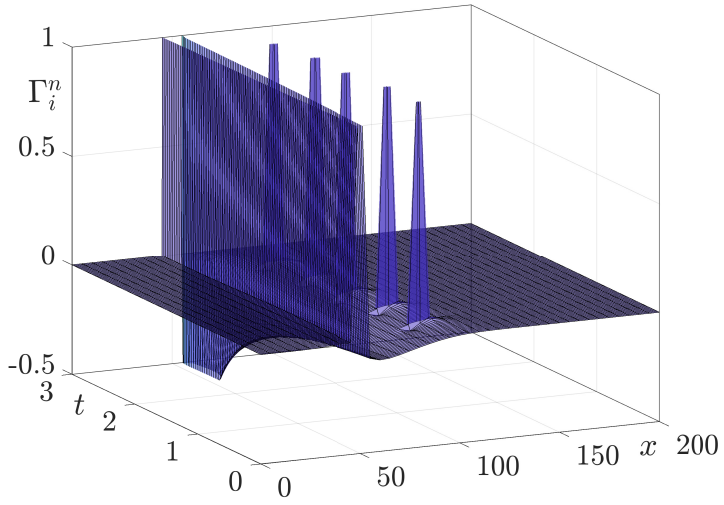

Figure 8. Γ surface of ELS at each early redemption dates and until maturity under specific conditions and its corresponding conditioned price.

Figure 8 shows the profile of the Γ value. As the maturity date approaches, and the underlying asset is near the knock-in barrier, Γ takes on positive values. In contrast, at each early redemption date or when the underlying asset price is around S_0, Γ tends to have negative values. When Γ takes on significantly negative or positive values, Δ becomes more sensitive to changes in the price of the underlying asset. For this reason, it can be inferred from Figure 7 that the Δ value responds sensitively when the underlying asset is near the knock-in barrier.

3.3. Theta (Θ)

The fluctuation in the value of a portfolio as time t increases is measured by Θ, which is algebraically defined as the partial derivative of the option value with respect to time. We use the central difference method to calculate Θ as follows:

$$\Theta_i^n = \left(\frac{\partial u}{\partial t}\right)_i^n = \frac{u_i^{n+1} - u_i^{n-1}}{2\Delta t}.$$

Figure 9 displays the Θ profile and the Θ surface over time, respectively. The Θ value is generally negative because the value of an option tends to decrease over time as it approaches maturity.

3.4. Vega (ν)

The rate at which option prices fluctuate due to the volatility of the underlying assets is denoted by ν. Some option values may be sensitive to variations in volatility, and ν plays an important role in monitoring markets that are particularly vulnerable to volatility. We discretize ν using the central difference method for numerical computation as follows:

$$\nu_i^n = \left(\frac{\partial u}{\partial \sigma}\right)_i^n = \frac{u_i^n(\sigma + \Delta\sigma) - u_i^n(\sigma - \Delta\sigma)}{2\Delta\sigma},$$

where $\Delta\sigma = 0.01$ is the size of increment of volatility we used.

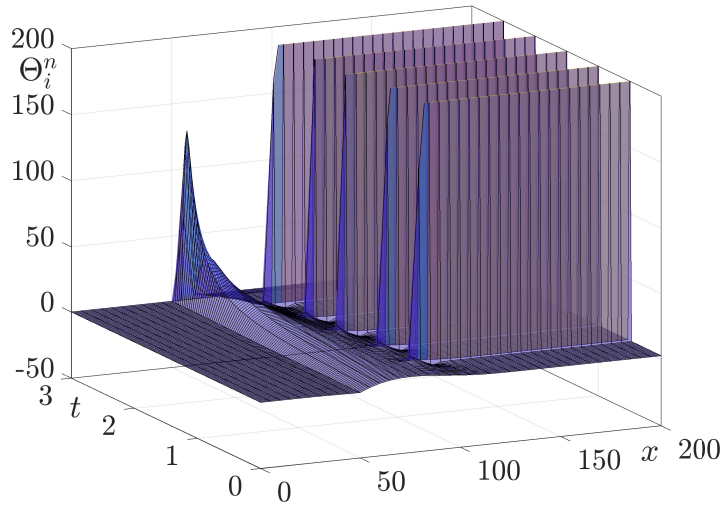

Figure 9. Θ surface of ELS at each early redemption dates and until maturity under specific conditions and its corresponding conditioned price.

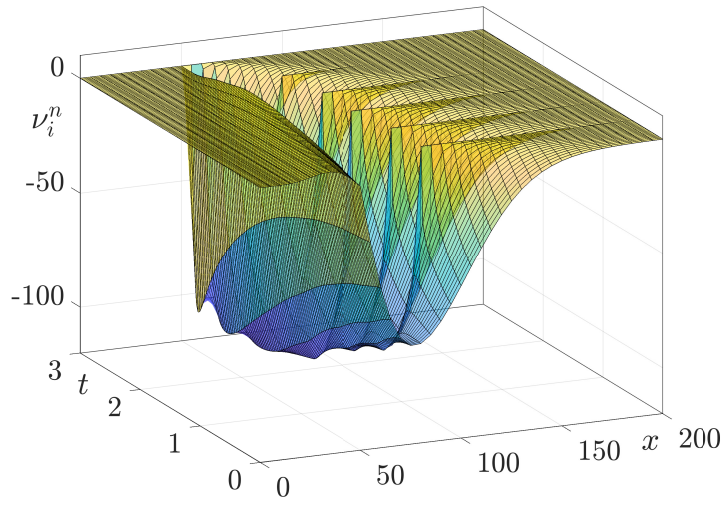

Figure 10. ν surface of ELS at each early redemption dates and until maturity under specific conditions and its corresponding conditioned price.

Figure 10 shows the profile of the ν value. The ν value is large and negative when the underlying asset is near the knock-in barrier and as the redemption date approaches maturity. At each redemption point, the ν value first increases and then decreases. A large absolute ν indicates high sensitivity to changes in volatility. When hedging ν, it is crucial to take into account both the time intervals between rebalancing events and the fluctuations in volatility.

3.5. Rho (ρ)

The sensitivity of the option price to variations in the risk-free interest rate is quantified by ρ. A high ρ means that the change in interest has a high impact on the option price. Applying the second order central difference method, ρ can be calculated on the computational grid.

$$\rho_i^n = \left(\frac{\partial u}{\partial r}\right)_i^n = \frac{u_i^n(r+\Delta r) - u_i^n(r-\Delta r)}{2\Delta r}. \tag{15}$$

where $\Delta r = 0.001$ is the size of increment for ρ we used.

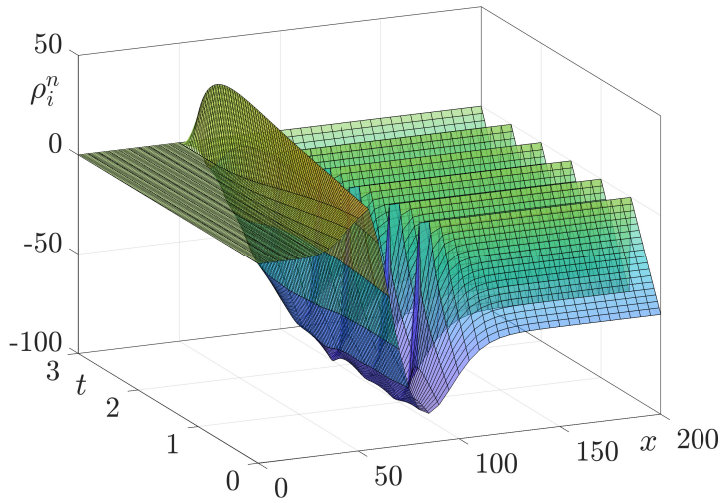

Figure 11. ρ surface of ELS at each early redemption dates and until maturity under specific conditions and its corresponding conditioned price.

Figure 11 shows the ρ surface. Regardless of the redemption point, ρ takes a positive value within the knock-in barrier range. As the price of the underlying asset increases, ρ rapidly decreases and becomes a large negative value. As the underlying asset price approaches S_0, ρ starts to increase again and eventually tends toward zero. Similar to ν, ρ increases sharply as the redemption point approaches and then decreases rapidly.

4. Evaluating the appropriateness of ELS in different scenarios

Finally, we calculate the values of different structural ELS products. Unlike the payoffs in Equations (1) and (2) discussed above, we consider an ELS product with the following payoff. If the knock-in barrier is touched,

$$v(S, T_i) = \begin{cases} F(1 + c_6), & \text{if } S \geq K_6, \\ 0.5F(S + K_6)/S_0, & \text{otherwise}, \end{cases} \tag{16}$$

if the knock-in barrier is not touched,

$$u(S,T_i)=\begin{cases}F(1+c_6), & \text{if } S\geq K_6,\\ F(1+d), & \text{if } D<S<K_6,\\ 0.5F(S+K_6)/S_0, & \text{otherwise.}\end{cases} \tag{17}$$

The payoff described above differs from the previously discussed payoffs in Equations (1) and (2) in that it provides a constant profit even if the value of the underlying asset S becomes 0 at maturity. See Figure 12.

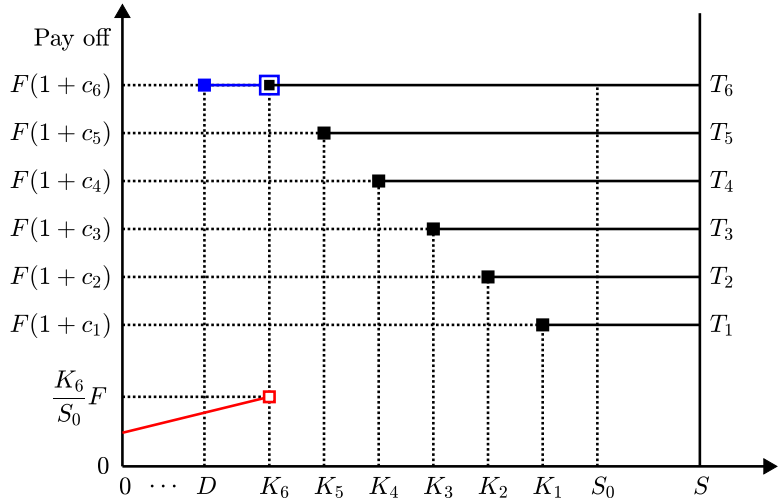

Figure 12. Payoff function for the early redemption date across different scenarios.

When $S=0$ for products whose future profit is 0, it is calculated using the zero Dirichlet boundary at $i=1$. However, when $S=0$ for products whose future profit is not 0, the discounted price of the future profit must be considered at $i=1$. In this case, either the Dirichlet boundary for the discounted value at $i=1$ or the linear boundary can be applied. The values and Greeks of ELS calculated by applying the linear boundary are consistent with previous results. Figure 13 shows the values and Greeks of ELS products calculated by applying linear boundary to payoff Equations (16) and (17). The parameters used in this computational test are the same as in Table 1.

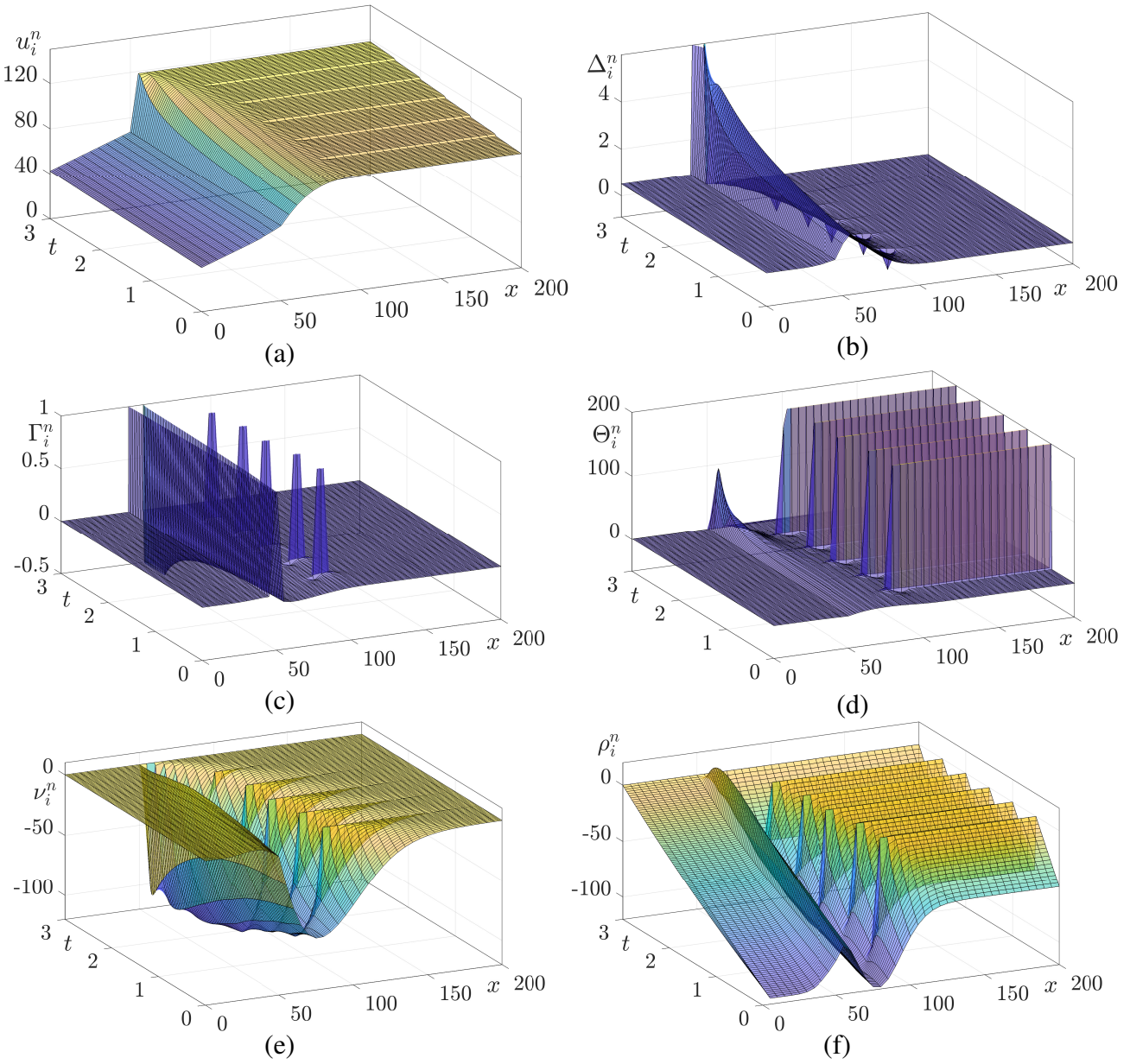

Figure 13. Numerical price and Greeks for payoffs in Equations (1) and (2).

5. Conclusions

In this study, we developed a computational method for the accurate computation of the option prices and Greeks for the ELS near early redemption dates. We used the BS equation and FDM to compute the ELS price and its Greeks. The proposed method solved the BS equation at early redemption dates using the Dirichlet boundary condition at strike prices instead of overwriting the option values on greater than or equal to strike prices by the given option prices. As a result, we observed that our computing algorithm is precise and useful for ELS pricing and its Greeks close to each early redemption date and the maturity time. Greeks have been measured to hedge the risk of derivative products, and Greeks hedging can be applied to manage the risk of ELS products. The computation of Greeks of ELS not only provides better hedging strategies for the finance industry but also facilitates risk- reduction decisions. For future research, a higher-order numerical scheme, such as the Crank–Nicolson method (Roul and Goura, 2020), can be applied to improve the accuracy of time discretization. Moreover, machine learning techniques should be explored to enhance both the efficiency and accuracy of numerical methods. For instance, machine learning approaches should be considered for optimizing hedging strategies based on dynamically changing market conditions (Wang and Yan, 2023). Additionally, deep learning-based surrogate models can be developed to approximate option price surfaces efficiently, which reduces computational costs while maintaining precision (Anderson and Ulrych, 2023).

Author contributions

Yunjae Nam: Conceptualization, Data curation, Resources, Formal analysis, Software, Visualization, Writing – original draft, and Writing – review & editing. **Changwoo Yoo:** Formal analysis, Resources, Data curation, Validation, and Writing – original draft. **Hyundong Kim:** Validation, Formal analysis, Resources, Investigation, Visualization, and Writing – review & editing. **Jaewon Hong:** Validation, Investigation, Data curation, and Writing – original draft. **Minjoon Bang:** Validation, Investigation, Data curation, and Writing – review & editing. **Junseok Kim:** Conceptualization, Supervision, Project administration, Funding acquisition, Formal analysis, Resources, Methodology, Writing – original draft, and Writing – review & editing.

Use of AI tools declaration

This article was not created using Artificial Intelligence (AI) tools.

Acknowledgments

This work was supported by the National Research Foundation (NRF), Korea, under project BK21 FOUR. The authors are grateful to the reviewers for their insightful and constructive feedback.

Conflicts of Interest

The authors declare no conflict of interest in this paper.

References

Anderson D, Ulrych U (2023) Accelerated American option pricing with deep neural networks. *Quant Financ Econ* 7: 207–228. https://doi.org/10.3934/QFE.2023011

Black F, Scholes M (1973) The pricing of options and corporate liabilities. *J Polit Econ* 81: 637–654. https://doi.org/10.1086/260062

Cui Y, Li L, Zhang G (2024) Pricing and hedging autocallable products by Markov chain approximation. *Rev Deriv Res* 27: 1–45.

Hwang Y, Kim I, Kwak S, et al. (2023) Unconditionally stable monte carlo simulation for solving the multi-dimensional Allen–Cahn equation. *Electron Res Arch* 31. https://doi.org/10.3934/era.2023261

Jo J, Kim Y (2013) Comparison of numerical schemes on multi-dimensional Black–Scholes equations. *Bull Korean Math Soc* 50: 2035–2051. https://doi.org/10.4134/BKMS.2013.50.6.2035

Kanamura T (2018) Diversification effect of commodity futures on financial markets. *Quant Financ Econ* 2: 821–836. https://doi.org/10.3934/QFE.2018.4.821

Kim ST, Kim HG, Kim JH (2021) ELS pricing and hedging in a fractional Brownian motion environment. *Chaos Solitons Fractals* 142: 110453. https://doi.org/10.1016/j.chaos.2020.110453

Kwak S, Kang S, Ham S, et al. (2023) An unconditionally stable difference scheme for the two-dimensional modified Fisher–Kolmogorov–Petrovsky–Piscounov equation. *J Math* 2023: 5527728. https://doi.org/10.1155/2023/5527728

Larguinho M, Dias JC, Braumann CA (2022) Pricing and hedging bond options and sinking-fund bonds under the CIR model. *Quant Financ Econ* 6: 1–34. https://doi.org/10.3934/QFE.2022001

Lee H, Ha H, Kong B, et al. (2024) Valuing three-asset barrier options and autocallable products via exit probabilities of Brownian bridge. *N Am Econ Financ* 73: 102174. https://doi.org/10.1016/j.najef.2024.102174

Lee C, Kwak S, Hwang Y, et al. (2023) Accurate and efficient finite difference method for the Black–Scholes model with no far-field boundary conditions. *Comput Econ* 61: 1207–1224. https://doi.org/10.1007/s10614-022-10242-w

Liu T, Li T, Ullah MZ (2024) On five-point equidistant stencils based on Gaussian function with application in numerical multi-dimensional option pricing. *Comput Math Appl* 176: 35–45. https://doi.org/10.1016/j.camwa.2024.09.003

Liu T, Soleymani F, Ullah MZ (2024) Solving multi-dimensional European option pricing problems by integrals of the inverse quadratic radial basis function on non-uniform meshes. *Chaos Solitons Fractals* 185: 115156. https://doi.org/10.1016/j.chaos.2024.115156

Lyu J, Park E, Kim S, et al. (2021) Optimal non-uniform finite difference grids for the Black–Scholes equations. *Math Comput Simul* 182: 690–704. https://doi.org/10.1016/j.matcom.2020.12.002

Roul P, Goura VP (2020) A sixth order numerical method and its convergence for generalized Black–Scholes PDE. *J Comput Appl Math* 377: 112881. https://doi.org/10.1016/j.cam.2020.112881

Tao L, Lai Y, Ji Y, et al. (2023) Asian option pricing under sub-fractional Vasicek model. *Quant Finan Econ* 7: 403–419. https://doi.org/10.3934/QFE.2023020

Thomas L (1949) Elliptic Problems in Linear Differential Equations Over a Network: Watson Scientific Computing Laboratory. Columbia University: New York, NY, USA

Wang Y, Yan K (2023) Machine learning-based quantitative trading strategies across different time intervals in the American market. *Quant Financ Econ* 7: 569–594. https://doi.org/10.3934/QFE.2023028

Wu X, Wen S, Shao W, et al. (2023) Numerical Investigation of Fractional Step-Down ELS Option. *Fractal Fract* 7: 126. https://doi.org/10.3390/fractalfract7020126

AIMS Press